PHYSICAL REVIEW B VOLUME 26, NUMBER 6 15 SEPTEMBER 1982

Oxygen adsorption on the indium antimonide (110) surface

Victor M. Bermudez and Victor H. Ritz
Naval Research Laboratory, Washington, D.C. 20375
(Received 19 March 1982)

The formation and structure of the natural oxide on UHV-cleaved InSb(110) surfaces are studied using ultraviolet photoemission spectroscopy (UPS), electron-energy-loss spectroscopy (ELS), and spectroscopic ellipsometry ($1.5 < h\nu < 4.5$ eV). The exposure of the as-cleaved surface to small amounts of O_2 [~ 30 L (1 Langmuir $= 10^{-6}$ Torr sec)] causes a slight rearrangement of surface atoms leading to changes in the shape of the upper valence band and in the surface optical dielectric function. Increasing O_2 exposure causes oxide formation which is first detectable (as a chemical shift in the In $4d$ UPS) at $\sim 10^5$ L. The oxide growth is spatially uniform, and the first monolayer is complete by approximately 10^6 L. Overall, the oxide is a mixture of In and Sb oxides and is a good insulator. The outermost surface of the oxide appears to be Sb rich. ELS transitions involving intrinsic surface states are observed in the oxide and possibly also on the clean surface.

I. INTRODUCTION

For most of the III-V semiconductors, much attention has been given to the properties of the clean surfaces and of the oxide and metal interfaces. However, less work has been done on the narrow band-gap materials (i.e., InAs and InSb) because of the limited energy resolution of the conventional surface-sensitive techniques of electron spectroscopy. The purpose of the work reported here is to contribute to the basic understanding of the room-temperature natural oxide on InSb. Surface-sensitive spectroscopic ellipsometry will be employed in conjunction with ultraviolet photoemission spectroscopy (UPS) and electron-energy-loss (ELS) spectroscopy. Our interest in this problem is motivated in part by the increasing use of infrared-sensitive materials in metal-oxide-semiconductor (MOS) devices such as detector arrays and imaging systems.[1] Although such components use SiO_2 as the insulating layer, a natural oxide film a few tens of angstroms thick is present on the substrate before passivation. This natural oxide layer remains at the interface, although the structure and composition may be modified by the oxide deposition.[2] Careful passivation[1,2] of the InSb($\bar{1}\,\bar{1}\,\bar{1}$) natural oxide (by low-temperature chemical vapor deposition of SiO_2) has resulted in interface-state densities of $< 5 \times 10^{10}$/eV cm^2.

InSb crystallizes in the ZnS (zinc blende) structure and cleaves along the (110) plane to give a stable (1×1) surface.[3] Other surfaces can be prepared by orienting and cutting, followed by ion bombardment and annealing in UHV (Refs. 3–5); however, these treatments may yield a damaged surface.[6] Recently Meyer *et al.*[7] have reported quantitative low-energy electron diffraction (LEED) structural analyses of the InSb(110) surface relaxation.

Eastman and Freeouf[8] have reported the valence-band UPS of InSb in the $20 \leq h\nu \leq 70$ eV range of photon energies and found that $h\nu \geq 40$ eV is sufficient to reveal all the structure in the density of states. Several UPS and x-ray photoelection spectroscopy (XPS) studies[8–11] have been reported in connection with the bulk band structure of InSb, but no surface effects have been noted in these investigations. XPS and also Auger-electron spectroscopy (AES) have provided some information on the chemical composition of thick natural-oxide layers from the chemical shifts of the In and Sb $3d$ core levels and of the In and Sb $M_{4,5}N_{4,5}N_{4,5}$ AES transitions. Samples prepared by polishing and etching the (111) (In-rich A) and ($\bar{1}\,\bar{1}\,\bar{1}$) (Sb-rich B) faces,[12] by cleaving in dry argon[13] or by Ar^+-ion bombardment of the (111) surface[14] form an oxide in dry O_2 at room temperature consisting of In_2O_3 and either Sb_2O_3 (Refs. 12 and 13) or a complex mixture of Sb_2O_3 and Sb_2O_5.[14] Oxidation in "wet" O_2 or in oxygen excited by a Tesla discharge yields Sb_2O_5 which loses O_2 to form Sb_2O_3 during annealing or x irradiation.[13,14] The composition of the natural oxide on a chemically cleaned ($\bar{1}\,\bar{1}\,\bar{1}$) surface is thought[15]

to be In_2O_3 and Sb_2O_3 in a 3:1 ratio. The presence of defects influences the rate of oxidation of InSb surfaces,[16] particularly those prepared by ion bombardment. Recently, Wilmsen[17] has reviewed the structure of thermal and anodic native oxides (but not room-temperature natural oxides) on the III-V compounds. UPS studies of Cl_2 adsorption have been performed on UHV-cleaved surfaces[18]; these show that chlorination occurs preferentially at the Sb site.

The surface-state structure of all the III-V compounds except InSb has been studied in the ELS experiments of van Laar *et al.*[19] and Huijser *et al.*[20] A model for InSb, inferred[19] by extrapolation of these data, is shown in Fig. 1 with surface-state levels labeled B_1, B_2, etc. The notation[19] corresponds to that used by Joannopoulos and Cohen[21] in their calculation of the unrelaxed GaAs(110) surface (see also Nishida, Ref. 22). Recently Schmeits *et al.*[23] have performed surface-state calculations specifically for the relaxed InSb(110) surface and their results are labeled D_a, D_c, etc. (a = anion, c = cation). No level was reported corresponding to the B_2' state of Joannopoulos and Cohen.[21] All calculations[21–23] have indicated the orbital compositions of the surface states, which are described qualitatively in Fig. 1. The classification into In and Sb orbitals is only approximate, since all surface states involve some contribution from both species. Also shown are the valence-band energy-distribution curve and upper core-level (In 4*d*, Sb 4*d*) binding energies reported by Eastman and Freeouf.[8] Thus far, only the B_1' state of InSb has been observed experimentally (by Eastman and Freeouf[24] using photoemission partial-yield spectroscopy). There is general agreement that, with the possible exception of GaP, intrinsic surface states on clean, ordered, and well-cleaved (see below) III–V (110) surfaces lie outside the band gap. For InSb this is confirmed by the ac field-effect measurements on UHV-cleaved surfaces by Kreutz *et al.*[25–27] A U-shaped distribution of fast intrinsic surface states is found with a minimum at midgap of $N_{ss} < 10^{13}$/eV cm^2. The exact shape and density near the band edges depends on the assumptions as to the scattering mechanism and surface carrier mobility made in analyzing the field-effect data, and the observed N_{ss} probably indicates residual imperfections on well-cleaved samples.

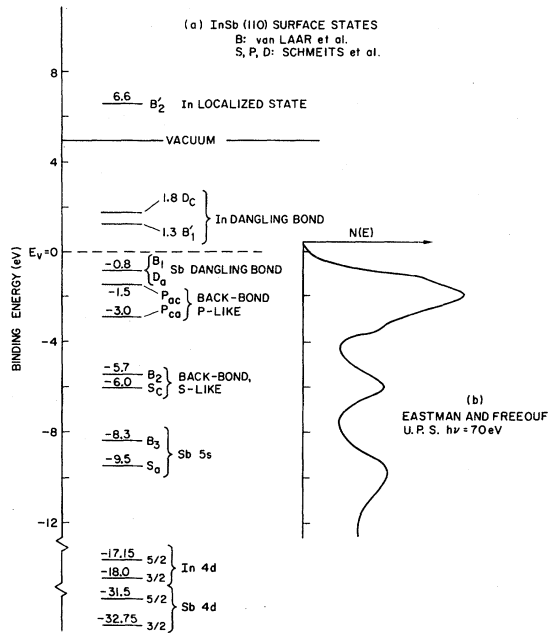

FIG. 1. InSb one-electron energy-level diagram. B_1, B_2, and B_3 are the occupied and B_1' and B_2' the unoccupied surface-state energies as estimated by van Laar *et al.* (Ref. 19) with reference to the unrelaxed GaAs(110) surface-state calculations of Joannopoulos and Cohen. (Ref. 21). The surface-state energies calculated by Schmeits *et al.* (Ref. 23) for the relaxed InSb(110) surface are given. The descriptions of the states (e.g., Sb dangling bond) are based on the reported (Refs. 21–23) orbital compositions. The core-level binding energies and valence-band energy-distribution curve observed in the photoemission experiments ($h\nu$=70 eV) of Eastman and Freeouf (Ref. 8) are also shown.

There is further general agreement that nonideal (110) surfaces have a significant density of surface states in the band gap. This has been extensively documented for GaAs.[28–31] Nonidealities take the form of physical imperfections (strain, steps, "tear marks"[28]) or adsorbates. The mechanism leading to these extrinsic or defect surface states is not clear. Lüth *et al.*[28] suggest that imperfections prevent reconstruction of the ideally terminated surface, a process which is responsible for eliminating surface states in the band gap. Kreutz *et al.*,[25–27] in discussing their InSb field-effect measurements, associate states in the band gap with cleavage-induced strain and surface irregularities which are especially pronounced for "bad" cleaves. Strain is believed to cause a "tailing" of bulk and intrinsic surface states into the surface band gap through the introduction of spatially random fluctuations in the surface potential. For bad cleaves, surface point defects generate a pronounced peak in the density of states in the band gap.

The research reported here addresses several as-

pects of the oxidation of the InSb(110) surface. Several techniques will be employed to obtain information about the initial stages of oxide formation, the development of the InSb-oxide interface, and the composition and structure of the thick natural oxide.

II. EXPERIMENTAL DETAILS

All electron spectroscopy (AES, ELS, and UPS) was carried out using a double-pass cylindrical-mirror analyzer (CMA). AES were recorded in the unretarded first-derivative mode ($d[EN(E)]/dE$), ELS in the retarded first- or second-derivative modes [$dN(E)/dE$ or $-d^2N(E)/dE^2$] and UPS in the retarded pulse-count mode [$N(E)$]. Some UPS spectra were also obtained as $dN(E)/dE$ in a search for additional structure. The CMA coaxial electron gun was used for excitation in AES ($E_p = 3.0$ keV, $i_p = 2$ μA) and ELS ($50 \leq E_p \leq 1500$ eV, $0.7 \leq i_p \leq 4.0$ μA). The energy resolution in ELS, determined from the halfwidth of the elastic peak, was $0.8 \leq \Delta E \leq 1.0$ eV. The UPS excitation source was a differentially pumped dc-excited helium resonance lamp (Physical Electronics Ind. Model 04-180) operated at 300 mtorr so as to maximize the He II—to—He I intensity ratio. UPS binding energies are referenced to the Fermi level E_F. The choice of binding-energy reference (E_F or valence-band edge E_V) is not critical since the net UPS energy resolution ($E \lesssim 0.5$ eV) is greater than the InSb room-temperature band gap, 0.18 eV. A major difficulty in the UPS experiments was the presence of weak ghost lines[32] in the source spectrum at 48.4, 51.0, 52.2, and 52.9 eV. The strongest of these, at 48.4 eV, had an intensity of $\sim 9\%$ that of the main line at 40.8 eV, based on the appearance of the In 4d ghosts. The others exhibited about 3% of the main-line strength or less. On a clean InSb surface, the In 4d photoemission was sufficiently intense that the ghosts of this feature completely overwhelmed most of the valence-band emission. Hence, He II UPS data for the valence band are presented only for oxidized samples in which the In 4d intensity is diminished, with respect to that of the oxide valence band to the point where simple numerical correction for ghost effects is practical. Since carbon accumulation on the clean surface was observed (in AES) to occur rapidly during irradiation by the primary beam, all experiments (other than ELS) were carried out prior to any exposure of the sample to electron beams. In ELS data were obtained on several freshly-cleaved samples with the use of the minimum possible electron irradiation. At the end of each set of experiments AES was used to check the surface condition. Samples used solely for UPS showed a carbon contamination of about 10 at. %. Extensive ELS experiments resulted in a doubling of this carbon level. Data were digitized with signal averaging and transferred to paper tape for off-line computer processing by means of a Nicolet 1072 Instrument Computer.

The ellipsometric measurements were made with a polarization-modulation system described previously.[33–35] With appropriate combinations of optical components, the system is capable of operation in the $1.4 \leq h\nu \leq 6.0$ eV range, although, the work reported here is concentrated on the 1.5—4.5 eV range. The source was a 1000-W Xe arc (with the necessary filters to remove infrared, stray light, and overlapping grating orders) coupled with a $\frac{1}{4}$-m monochromator (Jarrell-Ash 82-410) and a cooled photomultiplier (EMI 9558QA,S20 photocathode). The polarizer and analyzer were MgF_2 Rochon prisms. All measurements involved two-zone averaging[34] to reduce systematic error, with a correction applied for entrance-window birefringence. The angle of incidence was 61.8°. The accuracy of the spectroscopic experiment has previously been found[35] to be such that the real (n) and imaginary (k) indices of a dielectric material (KCl) can be obtained to within better than ± 0.002 in the visible and near uv. The energy resolution was approximately 10 meV (80 meV) at the low- (high-) energy end of the spectrum.

Single-crystal boules of InSb were provided by E. M. Swiggard (Naval Research Laboratory). Samples were prepared by x-ray orientation and cutting into a shape convenient for cleaving in UHV ($\sim 6 \times 6 \times 12$ mm^3 with the [110] axis parallel to the long edge). A notch cut perpendicular to the [110] axis facilitated cleaving by the chisel-and-anvil technique. All samples were cleaved at base pressures of below 2×10^{-10} Torr (4×10^{-10} Torr in ellipsometry experiments), and all experiments were done at room temperature. All experiments other than ellipsometry were done with nominally undoped samples. Based on the availability of samples, ellipsometric measurements employed Se-doped n-type material with a 77-K carrier density of about $2-8 \times 10^{15}$/cm^3. The quality of the cleavage obtained in different experiments will be noted where appropriate.

Research-purity O_2 (99.99%) was used in all experiments. Exposures of 10^6 L or less (1 L = 1 langmuir = 10^{-6} Torr sec = 3.59×10^{14}/ cm^2 O_2

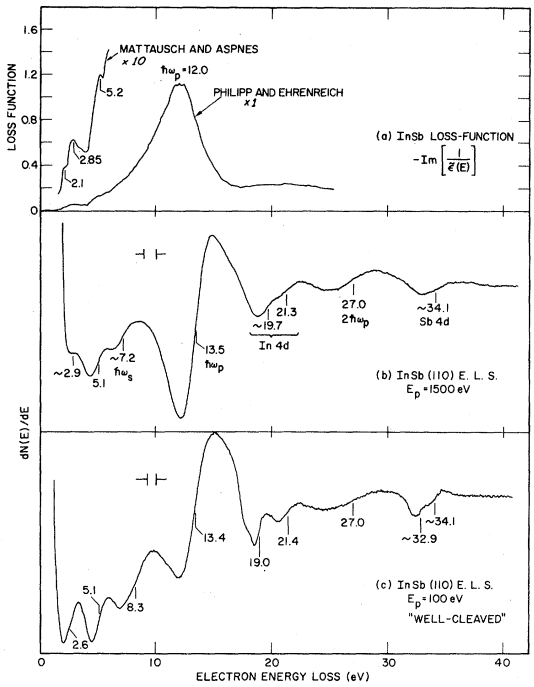

FIG. 2. (a) Bulk energy-loss function $-\mathrm{Im}[1/\tilde{\epsilon}(E)]$ computed from the dielectric function, $\tilde{\epsilon}=\epsilon_1+i\epsilon_2$, as measured optically by Philipp and Ehrenreich (Ref. 38) and by Mattausch and Aspnes (Ref. 39). First-derivative ELS ($E_p=1500$ eV) for UHV-cleaved InSb(110). The bulk ($\hbar\omega_p$) and surface ($\hbar\omega_s$) plasmons and the core-level excitations are indicated. (c) ELS at $E_p=100$ eV for a well-cleaved surface (see text).

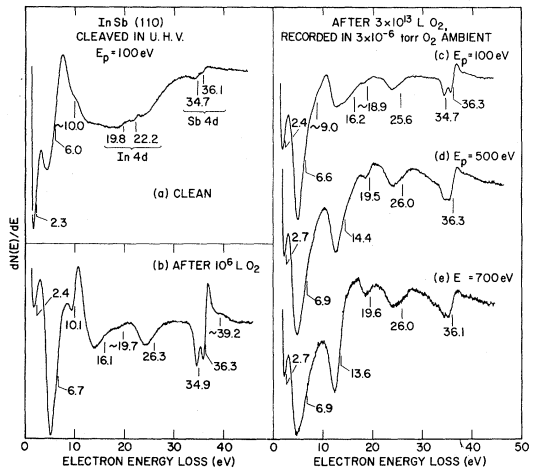

FIG. 3. (a) and (b) ELS of UHV-cleaved InSb(110) at $E_p=100$ eV before and after a 10^6-L exposure to excited O_2. (c)–(e) ELS of a heavily oxidized sample (3.1×10^{13} L) at $E_p=100$, 500, and 700 eV in a background of 3×10^{-6} Torr O_2.

fluence at 300 K) were carried out using either a nude (UPS, ELS) or a glass-encased (ellipsometry) Bayard-Alpert ionization gauge. The ion pump was turned off during backfilling of the chamber with O_2. The nude gauge operated at 0.8-mA emission current and the enclosed gauge at 10 mA. Although the hot filament was well out of a direct line of sight to the sample in either case, we consider these exposures to involve "excited oxygen" based on the work of Pianetta *et al.*[36,37] on gauge effects in the oxidation of GaAs. Exposures in excess of 10^6 L were performed using various thermocouple gauges at pressures of 10^{-3} Torr or more. In this case all cables were disconnected from the CMA since batteries in the control unit provide several hundred volts, even when the controller is switched off, and can initiate a plasma discharge at certain O_2 pressures. Although the O_2 is not excited in this case, these high exposures always followed smaller exposures to excited oxygen, and the ion pumps used during reevacuation were a potential source of excitation.

III. RESULTS AND DISCUSSION

A. ELS

The ELS results are summarized in Table I. Figure 2(a) shows the volume loss function $-\mathrm{Im}[1/\tilde{\epsilon}(E)]$ computed from the optically determined[38,39] dielectric function. The ELS for two different samples (both cleaved in UHV) are shown in Figs. 2(b) and 2(c). The spectrum in Fig. 2(b) at $E_p=1500$ eV is for a "less well-cleaved" specimen, with smaller areas of smooth, mirrorlike finish and a greater number of visible imperfections (i.e., steps and rough areas). We observe interband transitions at about 2.9 and 5.1 eV and the volume plasmon at $\hbar\omega_p=13.5$ eV. These results are in good agreement with the optical data. The lower value of $\hbar\omega_p$ obtained optically may result from uncertainty in reducing the reflectance data,[38] since transmission ELS (Ref. 40) at $E_p=50$ keV gives $\hbar\omega_p=13.0$ eV. In $4d$ and Sb $4d$ core-level transitions are found near 20 and 35 eV, respectively. A double plasmon loss occurs at $2\hbar\omega_p=27.0$ eV. A loss feature is observed at about 7.2 eV which gains intensity with decreasing E_p and becomes the dominant loss at $E_p\lesssim300$ eV (Second-derivative ELS gives the peak position more accurately as 6.7 eV at $E_p=300$ eV.) This transition is assigned to the surface plasmon. At $E_p=100$ eV, the spectrum shown in Fig. 3(a) is obtained for a less-well-

TABLE I. InSb electron-energy-loss transitions.

Clean surface[a]		Oxidized surface[b]	
2.6 eV	Interband	2.4 eV	Intrinsic surface state
5.1		6.7	Interband
8.3	Surface plasmon[c]	~10.1	Intrinsic surface state
13.5	Bulk plasmon	~16.1	Plasmon(?)
19.0	In $4d \rightarrow$ conduction band	19.7	In $4d$ exciton
21.4		26.3	O $2s \rightarrow$ conduction band
27.0	Double bulk plasmon	34.9	Sb $4d$ exciton (satellite)
~32.9	Sb $4d \rightarrow$ conduction band (bulk)	36.3	
~34.1		(~39.2)	
~34.7	Sb $4d \rightarrow B_2'$ (surface)[d]		
~36.1			

[a]Figure 2(c).
[b]Figure 3(b).
[c]Energy and intensity depend on cleavage quality (see text).
[d]Figure 3(a).

cleaved sample.

Figure 2(c) shows typical ELS data obtained at $E_p = 100$ eV for a "well-cleaved" surface, one with large mirror-smooth areas and a relatively small density of visible imperfections. This spectrum shows prominent bulk features, particularly the volume plasmon, and resembles (with better resolution) spectra obtained with less well-cleaved samples at $E_p \sim 1500$ eV. For well-cleaved crystals, the bulk plasmon is readily observable even with E_p as small at 50 eV and is the dominant feature at $E_p \gtrsim 500$ eV. We also note that the surface-plasmon energy is somewhat larger on well-cleaved surfaces, $\hbar\omega_s \sim 8.2$ eV. For all the other III-V compounds it is found[19] that $1.53 \leq \omega_p/\omega_s \leq 1.56$, which would suggest a value of $\hbar\omega_s \sim 8.7$ eV in InSb.

The dependence of the ELS on cleavage quality is attributed to variations in the local scattering geometry, i.e., a higher probability for near grazing-incidence events on an irregular surface, leading to a more intense surface-plasmon loss at low E_p. In Fig. 3(a) (irregular surface, low E_p) a very broad feature appears in the background with a peak at roughly 27 eV. Variation of E_p showed that this does not arise from diffracted slow-secondary electrons or from Auger emission. The feature is sensitive to oxidation [compare Figs. 3(a) and 3(b) below] and vanishes as E_p is increased [compare Figs. 2(b) and 3(a)]. It is not found in the low-E_p spectra for well-cleaved samples [Fig. 2(c)]. At present, we have no explanation for this effect.

Figure 3 shows the ELS for UHV-cleaved InSb before and after an excited oxygen exposure of 10^6 L. The data in Figs. 3(a) and 3(b) are for a less well-cleaved sample, and the clean-surface spectrum shows a strong surface plasmon and no bulk plasmon. Exposures beyond 10^6 L—up to 10^{13} L—resulted in no further change in the surface-sensitive ELS obtained at $E_p = 100$ eV. Data obtained at $E_p = 100$ eV in an O_2 ambient of 3×10^{-6} Torr were the same as those in Fig. 3(b), indicating that electron-stimulated desorption (ESD) of oxygen by the primary beam does not affect these data. Also, all peaks noted in Fig. 3(b), except the very weak In $4d$ features, were observed in the numerically integrated spectrum which rules out the presence of differentiation artifacts. The absence of Auger features in the ELS (for example, In $N_{2,3}VV$) was verified by comparing spectra obtained at $E_p = 89$ and $E_p = 100$ eV. *After O_2 exposures of 10^6 L or more, all samples yielded the same ELS at a given E_p, regardless of the nature of the clean-surface spectrum.*

The most striking effect of oxygen exposure is the increase in intensity of the Sb $4d$ transition, relative to that of the In $4d$. Figures 3(c)–3(e) show the ELS of a "thick" oxide as a function of E_p, prepared by exposing the sample (after 10^6 L of excited O_2) to a massive dose of unexcited O_2 (17 h at 510 Torr $= 3.1 \times 10^{13}$ L). The spectra were obtained in an O_2 background of 3×10^{-6} Torr to prevent ESD effects. Increasing E_p in the $100 \leq E_p \leq 700$ eV range results in a reduction of the Sb $4d$-to-In $4d$ intensity ratio, which approaches that of the clean substrate. For $E_p \gtrsim 500$ eV, the loss features arising from the substrate—most notably the volume plasmon—become apparent. These results cannot be explained in terms of a

dependence of the relative Sb 4*d*-to-In 4*d* scattering cross section on E_p or on oxidation, since the intensity ratio is independent of E_p (in the 100–1500-eV range) for clean InSb. Furthermore, there is no apparent increase in the ELS intensity of Sb 4*d* in the oxidation of Sb metal[41] to Sb_2O_3 or decrease in the In 4*d* intensity in the electron-stimulated oxidation of InP (Ref. 42) to In_2O_3. We conclude that the outermost layer of the natural oxide contains an excess of Sb (in an as-yet-unknown oxidation state). We caution that we cannot rule out the possibility that this stratification is caused in some way by the electron beam, possibly through preferential evaporation or diffusion. However, we observed no change in the ELS of heavily oxidized InSb during electron-beam irradiation. Soft x-ray photoemission ($h\nu \sim 80$ eV) would be helpful in determining the Sb-to-In ratio.

Two aspects of the Sb 4*d* ELS are of further interest. First, there is a clear and reproducible shift in the transition energy from ~34.1 eV in the bulk spectra [Figs. 2(b) and 2(c)] to ~36.1 eV in the surface-sensitive data, Fig. 3(a), a shift of ~2.0 eV to *higher transition energy* in going from bulk to surface. On the other hand, Eastman *et al.*[43] have observed a shift of 0.36 eV to *lower binding energy* on going from bulk to surface for the Sb 4*d* level of GaSb(110). Assuming the same Sb 4*d* shift in InSb, one infers from the data a large ELS final-state shift in going from bulk to surface. Using the surface Sb $4d_{3/2}$ binding energy (32.75 eV, Fig. 1) and the Sb $4d_{3/2}$ surface-ELS transition energy (~36.1 eV), we obtain a (relaxed) final state ~3.4 eV above the valence-band edge (Fig. 1). Further assuming B_2' to be the final state of the surface ELS transition, we conclude that 3.4 eV above E_V represents a lower limit on the position of this state since the relaxation energy is not known. For In 4*d* the surface binding-energy shift is unknown, and the ELS energies are more difficult to determine precisely.

In Figs. 3(c)–3(e) the Sb 4*d* ELS feature is observed to broaden asymmetrically to lower transition energy with increasing E_p. This could possibly arise from variation in the Sb oxidation state with depth into the oxide, since the corresponding transition (unresolved doublet, $E_p = 500$ eV) in the metallic element[41] is at 34.1 eV vs 37.1 eV in Sb_2O_3 and 36.4 eV in Sb_2S_3. However, evidence will be presented below against the presence of a sizable concentration of elemental Sb in thick natural oxide films. The asymmetry is instead explained by the increasing contribution from the unoxidized InSb substrate, as revealed by the increasing loss intensity at $\hbar\omega_p$.

Other features in the clean [Fig. 3(a)] and oxidized [Fig. 3(b)] InSb surface ELS can now be discussed. This is complicated by the fact that structure in the bulk, clean-surface and oxidized-surface spectra are all mutually overlapping within the present resolution limits. Also, the bulk and oxidized-surface ELS both exhibit structure near the expected surface-state transition energies (Fig. 1), which means that such features cannot be positively identified on the basis of the dependence of the spectra on E_p or on oxidation.

The major feature in the clean-surface ELS [Fig. 3(a)] is the surface plasmon at ~6 eV. A peak is found at essentially the same energy, ~6.7 eV, in the oxidized surface. This is approximately midway between the interband transition[41] in Sb_2O_3 at 7.5 eV and that in heavily oxidized InP (Ref. 42) at

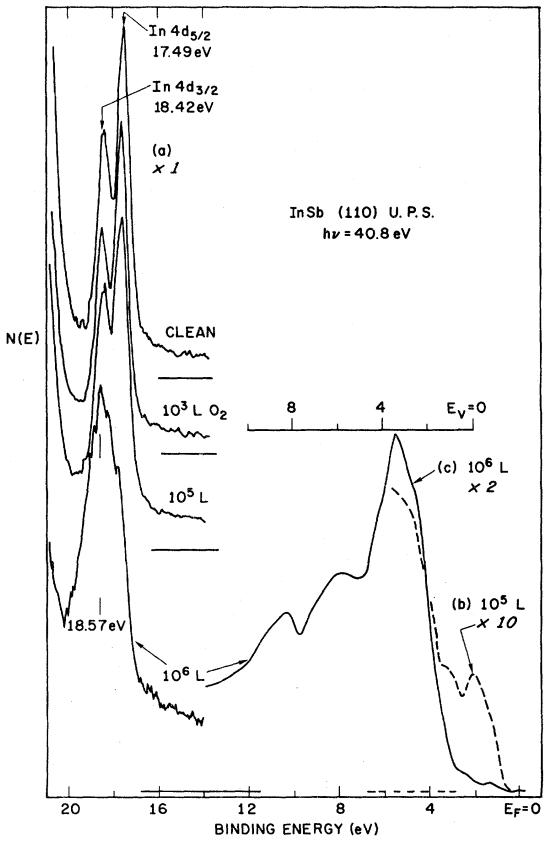

FIG. 4. (a) In 4*d* spin-orbit doublet of UHV-cleaved InSb for different excited-oxygen exposures. (b) Upper valence band after a 10^5-L excited-O_2 exposure. (c) Total valence-band density of states [corrected for In 4*d* ghosts (see text)] after 10^6-L O_2. The horizontal line below each spectrum gives the zero-count level.

5.9 eV. A broad feature is found at ~16 eV after oxidation; both Sb_2O_3 (Ref. 41) and In_2O_3 (Ref. 42) have loss structure in this energy range, possibly associated with plasmons in the oxides. From the oxide In $4d$ binding energy (16.5 eV below E_V, Fig. 4), the oxide ELS transition energy (19.7 eV), and the oxide band gap (~3.7 eV, see below), the In $4d$ ELS final state is located ~0.5 eV below the oxide conduction-band edge. This suggests an excitonic transition. The oxidation-induced loss at ~26 eV is assigned to an O $2s\rightarrow$ conduction-band transition, based on an O $2s$ binding energy of ~21 eV below E_V which is typical for metal oxides. We also note a very weak shoulder on the high-energy side of the Sb $4d$ (at ~39.5 eV) after oxidation, the assignment of which is uncertain. It may be a satellite [either shake up or double loss (involving the 2.4-eV loss)], or it may be the Sb $4d$ transition in a small concentration of Sb_2O_5.

Neither the 2.4 nor the 10 eV losses observed for the oxidized surface are found in the ELS of Sb_2O_3 (Ref. 41) or In_2O_3 (Ref. 42) and the former is substantially less than the band gap of either oxide (~4.3 and ~3.8 eV, respectively). Coincidentally, the 2.4 eV transition occurs close to the clean-surface transition at 2.3 eV. The 2.3 eV clean-surface peak occurs near the energy expected for the $B_1\rightarrow B_1'$ surface-state transition (see Fig. 1). Although it appears to shift slightly to higher loss energy with increasing E_p it cannot be definitively assigned to a surface-state process because of the limited energy resolution. A similar situation prevails for the 10-eV oxidized-surface peak. A weak shoulder is seen at ~10 eV for the clean surface, close to the anticipated $B_3\rightarrow B_1'$ and $B_2\rightarrow B_2'$ energies. However, increasing E_p beyond ~500 eV causes the volume plasmon to interfere with this part of the spectrum. The peaks at 2.4 and 10 eV in Fig. 3(b) are assigned to oxide surface states, the latter being not as well resolved in Fig. 3(c) as in Fig. 3(b). This is confirmed by the data in Figs. 3(c)-3(e), which show a decrease in the intensities of these features with increasing E_p for a thick oxide. Complete disappearance of the 2.4 eV peak at higher E_p is not to be expected since the InSb substrate contributes structure for $E_p \gtrsim 500$ eV.

B. UPS

Figure 4 shows the evolution of the In $4d$ photoemission with increasing excited-oxygen exposure. The clean-surface In $4d$ binding energy and spin-orbit splitting are in agreement with those of Eastman and Freeouf.[8] For the III-V compounds a pronounced oxygen adsorption effect on the cation core-level spectra indicates[36] formation of a surface oxide accompanied by breaking of the anion-cation chemical bond. Adsorption involving only dangling-bond surface states is expected to take place only at anion sites, at which the B_1 state is localized. The threshold excited-oxygen exposure for detectable oxide formation is about 10^5 L, in agreement with results obtained for GaAs,[36,37] InP,[44] and InAs.[45] This finding is also consistent with the excited-oxygen sticking coefficient, $s < 10^{-5}$, estimated from LEED measurements[3] on Ar^+-ion bombarded InSb(110) surfaces after mild annealing. After a 10^5-L excited-oxygen exposure, there is a small apparent decrease in the In $4d_{5/2}$-to-$4d_{3/2}$ intensity ratio, relative to the clean surface. This results from the onset of a chemically shifted In $4d$ doublet at higher binding energy in the oxide. An excited-oxygen exposure in excess of 10^6 L (up to 3×10^{13} L) results in a single broad In $4d$ UPS line at a binding energy of ~18.6 eV. The oxidation-induced shift of the center of gravity of the In $4d$, about 0.7 eV, is somewhat larger than that reported by Legare *et al.*,[14] 0.25 eV, for a thick natural oxide on InSb(111) using Al $K\alpha$ excitation.

The valence-band UPS after 10^5- and 10^6-L oxygen exposures are also shown in Fig. 4; the latter has been corrected for the In $4d$ ghosts. The spectrum after 10^9 L was also obtained in the $dN(E)/dE$ mode (50-eV pass energy, 1-V modulation), but no additional structure was observed in the derivative spectrum. After 10^5 L of excited O_2 (the threshold exposure defined above) the top of the clean-surface valence band is still readily apparent as a shoulder on the edge of the oxide valence band and extending up to E_F. Below 10^4 L, the spectrum within 4 eV of E_F (comprising the uppermost peak in the InSb density of states) is qualitatively similar to that of clean InSb (Fig. 1).

Some insight into the oxidation process can be gained from these results. First, the oxide grows uniformly rather than as islands. This is evident from the fact that—with increasing O_2 exposure—the clean-surface valence-band structure disappears soon after the In $4d$ photoemission indicates the onset of oxide formation. There is no indication of two coexisting phases at higher exposure. In particular, after excited-oxygen exposures in excess of 10^6 L, there is no indication of the clean-surface In $4d_{5/2}$ line, which would appear as a shoulder on the low-binding-energy side of the broad In $4d$ feature (Fig. 4). Second, the surface

oxide formed at exposures in excess of 10^6 L is a good insulator, as suggested by the position of the Fermi level near midgap. Figure 4 shows the top of the oxide valence band to be about 2.1 eV below E_F, and optical data (see below) give a band gap of from 3.6 to 3.8 eV for the surface oxide. From this we infer the absence of a significant concentration of donor or acceptor species (point defects, Sb metal, etc.) in the oxide. The oxide valence-band emission consists of three peaks at about 3.4, 5.9, and 8.3 eV below E_V (5.5, 8.0, and 10.4 eV below E_F) with the uppermost being the most intense in qualitative agreement with other oxidized III-V compounds.[36,37,44,45] The intense peak near E_V is derived from O $2p$ nonbonding orbitals. On the basis of the He I UPS data of Legare *et al.*[14] for clean and oxidized In and Sb, the peak at 8.3 eV below E_V can be associated with In-O bonding orbitals and that at 5.9 eV below E_V with Sb—O bonds. Thus, the valence-band UPS indicates the presence of both In and Sb oxides; although, a quantitative determination of the relative concentrations is not possible. It was noted that—as oxidation proceeds—the In $4d$ emission decreases in intensity relative to the valence band. This is consistent with (but does not prove) the depletion of In from the outermost oxide layer, since the O $2p$ photoemission cross section is probably larger than that of the InSb valence band.[36,37]

C. Ellipsometry

The experiment measures three quantities as functions of photon energy

$$N=\cos(2\psi)\ ,$$
$$S=\sin(2\psi)\sin\Delta\ , \tag{1}$$
$$C=\sin(2\psi)\cos\Delta\ .$$

The ellipsometric angles ψ and Δ are related to the complex amplitude reflection coefficients by

$$\tan\psi e^{i\Delta}=\tilde{r}_p/\tilde{r}_s\ , \tag{2}$$

where p (s) refers to polarization parallel (perpendicular) to the plane of incidence. Any two of the experimental terms may be combined to yield ψ and Δ, from which the complex dielectric function ($\tilde{\epsilon}=\epsilon_1-i\epsilon_2$) may be obtained (using the Fresnel relations) as

$$\begin{aligned}\epsilon_1&=n^2-k^2\\&=\sin^2\theta+\sin^2\theta\tan^2\theta\frac{(N^2-S^2)}{(1+C)^2}\ ,\\ \epsilon_2&=2nk=2\sin^2\theta\tan^2\theta\frac{NS}{(1+C)^2}\ ,\end{aligned} \tag{3}$$

where θ is the angle of incidence. The dimensions of the focused source-image incident on the sample ($\sim 1\times 3$ mm^2) were sufficiently small so that smooth, mirrorlike areas of the cleaved samples could be studied, regardless of the overall quality of the cleaves.

Figure 5(a) shows ϵ_1 and ϵ_2 for UHV-cleaved InSb(110), which are in good overall agreement with the results of Mattausch and Aspnes.[39] However, we obtain a somewhat larger value of ϵ_2 at the E_2 critical point ($\epsilon_2=22.0$ at $h\nu=3.85$ eV) than do Aspnes and Studna[46] for their best chemically etched surface, which gave $\epsilon_2=20.8$ at E_2. As explained by Aspnes *et al.*,[39,46] this small increase in the "apparent" ϵ_2 indicates a significantly "higher-quality" (i.e., film-free) surface for the UHV-cleaved samples. The apparent ϵ_2 is that which is obtained from Eq. (3) using ψ and Δ for a film-covered surface. In this context the term "film" applies to the net effect of microscopic roughness and adsorbed contaminants. An exposure of 10^{10} L of unexcited O_2 (equivalent to 15 sec in 1 atm. of pure O_2) reduced the apparent ϵ_2 to 19.7 at E_2.

Figure 5(b) shows $\Delta\epsilon_1$ and $\Delta\epsilon_2$ for an exposure of 15 L to excited O_2. $\Delta\tilde{\epsilon}$ is obtained by measuring ψ and Δ before and after exposure and iteratively solving the Fresnel relations appropriate to the three-phase system[35] (ambient/isotropic film/isotropic substrate). The magnitude of $\Delta\tilde{\epsilon}$ is arbitrary, since an assumed value (5 Å) was used for the "film thickness" in the numerical data reduction. This choice, which is a reasonable estimate of the "surface-state depth," affects only the magnitude of $\Delta\tilde{\epsilon}$ and not the spectroscopic structure. $\Delta\tilde{\epsilon}$ then represents the change in $\tilde{\epsilon}$ within a surface layer of the assumed thickness. The minimum detectable $\Delta\tilde{\epsilon}$ is about 20% of one ordinate scale division.

One first notes that a readily detectable ellipsometric effect is observed at an oxygen exposure which is at least 3 orders of magnitude smaller than that at which the In $4d$ photoemission begins to change. A similar effect was observed by Lüth *et al.*[28] in the oxidation of GaAs and by Matz and Lüth[47] in the adsorption of hydrogen on ZnO. The structure in $\Delta\epsilon_2$ is seen to fall rather close to

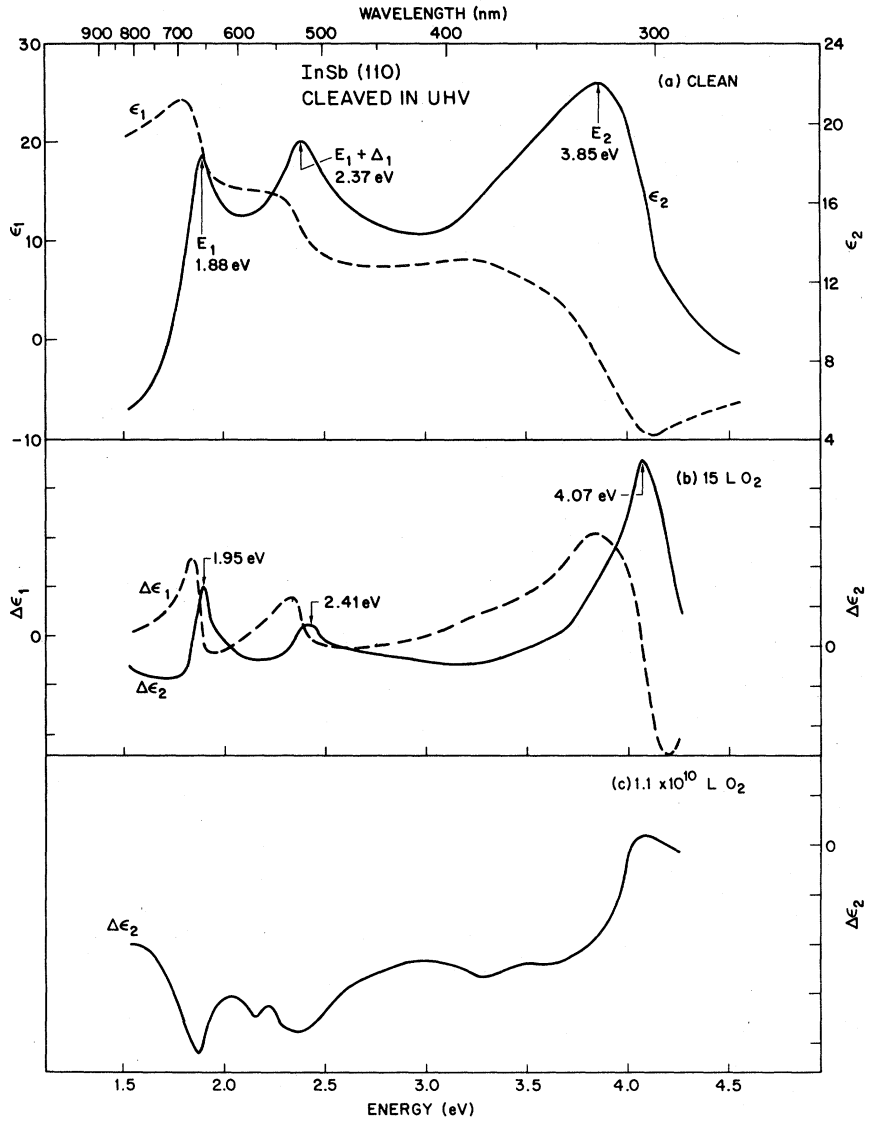

FIG. 5. (a) Real (ϵ_1) and imaginary (ϵ_2) dielectric functions of UHV-cleaved InSb(110), as determined ellipsometrically. E_1, $E_1+\Delta_1$, and E_2 label the bulk band-structure critical points. (b) Changes in ϵ_1 and ϵ_2 induced by a 15-L excited-O_2 exposure. Both ordinate scales are in the same arbitrary units (see text). (c) Change in ϵ_2 after a 1×10^{10}-L O_2 exposure. In both cases $\Delta\tilde{\epsilon}$ represents the change from the clean-surface quantity.

that in ϵ_2, especially at E_1 and $E_1+\Delta_1$. In the case of other compound semiconductors—GaAs,[28,48] GaP,[48,49] and ZnO,[47]—this result has been attributed mainly to the Franz-Keldysh effect in which the adsorbate dipole layer changes the surface band bending, producing structure similar to that in an electroreflectance spectrum. However, comparison of Fig. 5(b) with the InSb electroreflectance spectrum of Cardona *et al.*[50] shows that the structure at E_0' (3.16 eV) and at $E_0'+\Delta_0'$ (3.49 eV) in the latter is missing from the ellipsometric spectrum. Hence, it appears that the Franz-Keldysh effect cannot account for the present results. A second possible explanation is that the $\Delta\epsilon_2$ structure—which is mostly of a positive sign—is derived from the removal of surface states by oxygen adsorption. This model was proposed by Blanchet *et al.*[51,52] to account for the appearance of features related to bulk band-structure critical points in the differential reflectance data obtained for H_2, O_2, and CO on tungsten single-crystal surfaces. The sum rule[38]

$$\int_0^\infty \epsilon_2(\omega)d\omega = \pi\omega_p^2/2 \ , \tag{4}$$

(where ω_p is the plasmon frequency) requires that the decrease in ϵ_2, when optical transitions between surface states and resonances are eliminated by oxygen adsorption, be compensated by an increase in ϵ_2 for bulk and/or adsorbate-induced transitions. However, the effect shown in Fig. 5(b) seems to be complete at very low excited-O_2 exposures in the 10—30-L range. Higher exposures do not produce larger peaks in $\Delta\epsilon_2$, and the spectra gradually change to those characteristic of the oxidized surface, Fig. 5(c) (see below). For the case of InSb it seems unlikely that such small exposures are sufficient to remove all surface states, given that an exposure on the order of 10^5 L of excited oxygen is required for the observation of surface-oxide formation in the In 4*d* UPS. Reference to UPS studies[37,53] of oxygen adsorption on the GaAs(110) surface provides a reasonable explanation for the InSb results. It is found[37,53] that the energy-distribution curve in the upper part of the valence band is strongly cleavage dependent and that O_2 exposures of less than 100 L (and even prolonged standing in UHV) lead to a sharpening of structure in this part of the UPS to a degree dependent on the "quality" of the cleave. The nature of the cleave can be assessed independently by determining whether the Fermi level was pinned before oxygen adsorption. The effect of small O_2 exposure is believed[37,53] to be a cooperative, long-range relaxation of atoms on the imperfectly cleaved surface (which might also be termed "strain release"). No change in the LEED symmetry results from such a process.

To assess this explanation for the InSb ellipsometric results, the effect of a small (30 L) excited-oxygen exposure on the upper valence band was investigated using He I excitation, as shown in Fig. 6(a). At a few eV higher kinetic energy is the In 4*d* doublet, excited by the He II radiation also present in the source spectrum. This feature is very useful for normalization of the spectra. A clear change in the upper-valence-band shape is observed, similar to that found for GaAs,[37,53] which supports the above interpretation of the data in Fig. 5(b). Note that the shape change cannot result from oxide formation, since this would generate structure at >4 eV below E_F [see Fig. 4(b)]. Furthermore, with the previously estimated sticking coefficient of $s < 10^{-5}$, no features directly associated with adsorbed oxygen in any form would be detectable after a 30-L exposure. Figure 6(b) shows the UPS of a clean well-cleaved sample which exhibits sharper structure than either of the

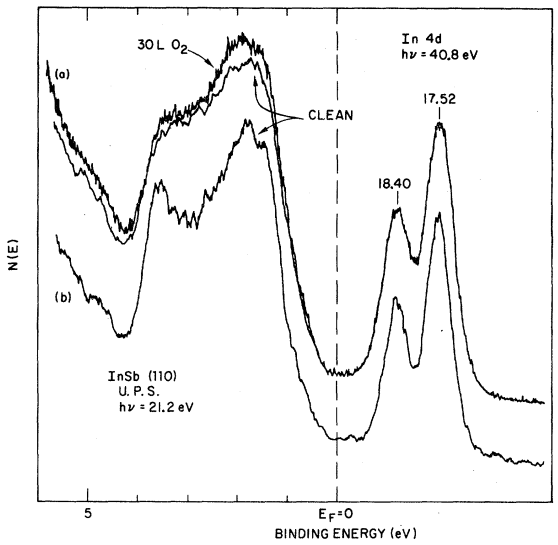

FIG. 6. (a) UPS of InSb(110), cleaved in vacuum before and after a 30-L excited-O_2 exposure. (b) UPS of a clean well-cleaved sample. The spectra consist of the upper valence band (see Fig. 1) excited by He I ($h\nu=21.2$ eV) and the In 4*d* core level excited by He II ($h\nu=40.8$ eV). The In 4*d* binding energies are indicated, and $E_F=0$ pertains to the He I spectrum.

spectra in Fig. 6(a) and demonstrates the cleavage dependence of $N(E)$ in the upper valence band. For the well-cleaved specimen, a 30-L excited-O_2 exposure has no effect other than a slight broadening of the shoulder at 1.5-eV binding energy.

To observe the ellipsometric effect of the oxygen itself (as opposed to adsorption-induced alteration of surface structure), much larger exposures are needed. Figure 5(c) shows $\Delta\epsilon_2$ after 1×10^{10} L of unexcited O_2. This quantity represents the average $\Delta\epsilon_2$ of the entire oxide layer, since the model used in data reduction assumes an isotropic overlayer and a sharp interface. There is a large overall displacement of $\Delta\epsilon_2$ to negative values, resulting from the presence of a well-defined oxide overlayer (see below) with a band gap of about 3.8 eV. Since ϵ_2 of the overlayer is essentially zero below the band edge, $\Delta\epsilon_2$ is negative, and the peaks at E_1 and $E_1+\Delta_1$ are in the negative direction. At about 3.6—3.8 eV, $\Delta\epsilon_2$ turns in the positive direction with a broad peak at about 4.1 eV. A positive-going peak in $\Delta\epsilon_2$ in this case can result only from a strong absorption in the oxide. In their study of thick (>1000 Å) anodic oxides on InSb, Mattausch and Aspnes[39] found a similar band edge which is close to that of In_2O_3 and about 0.5 eV lower than that in bulk Sb_2O_3. This is consistent

with the fact that the anodic oxide is known to be rich in In_2O_3 (except at the substrate interface).[17] With these data there is no indication of a second band edge (associated with Sb_2O_3) at higher energy, which may be obscured by the stronger In_2O_3 edge.

At this point some comment can be made as to the depth of the "thick" natural oxide. Previous estimates based on Auger and XPS sputter profiling[2] and on XPS chemical-etch profiling,[15] give values in the 15–25-Å range for the natural oxide on chemically cleaned $(\bar{1}\,\bar{1}\,\bar{1})$ surfaces. This range may define an upper limit since the experimental-depth resolutions are of about the same magnitude. ELS data, Figs. 3(c)–3(e), show an increase in the substrate bulk-plasmon intensity with E_p beginning at $E_p \lesssim 500$ eV. This is consistent with an oxide thickness of $\sim 20-25$ Å if one assumes an electron mean free path in the oxide of ~ 12 Å at 400-eV kinetic energy, as in SiO_2 and Al_2O_3.[54] Ellipsometric thickness estimates, based on the isotropic three-phase model with sharp interfaces, cannot be considered reliable in this particular case.

IV. CONCLUSIONS

Little information has been obtained about the clean surface because of the limited energy resolution available in the present ELS and UPS experiments and because of ghost lines in the He uv source. However, considerable understanding of the oxidation process has been derived. With regard to the clean surface, we have observed a large (~ 2 eV) dependence on E_p of the energies of ELS transitions from the Sb $4d$ core-level doublet. This has been interpreted in terms of a shift of the final state on going from bulk to surface. Assuming B_2' to be the final state for the surface ELS transition (B_1' is too close to the conduction-band edge), a lower limit of 3.4 eV is estimated for the energy of B_2' above the valence-band edge (see Fig. 1).

Optical spectroscopy shows that surfaces prepared by cleaving in UHV are noticeably better (i.e., more nearly free of extraneous films) than the best chemically cleaned specimens. Initial O_2 exposure causes a structural rearrangement of the surface (strain release) as revealed by changes in the shape of the upper valence-band UPS and in the surface-optical dielectric function. Increasing O_2 exposure leads to oxide formation which is first detectable (in the In $4d$ photoemission) at about 10^5 L. The oxide growth is spatially uniform, and the first monolayer is complete by approximately 10^6 L. Overall, the oxide is a mixture of In and Sb oxides—probably In_2O_3 and Sb_2O_3, which are the most stable forms. Compound formation is also, in principle, a possibility[55]; although, there is no clear indication in this or in earlier work of such a process in the room-temperature formation of the natural oxide. The outermost oxide layer is enriched in Sb (depleted of In) as inferred from ELS and partially supported by UPS data. It is possible that the excess Sb oxide on the surface might be an artifact of the ELS primary electron-beam irradiation. Earlier studies[2,12–15] of InSb oxidation, based on observation of the In and Sb $M_{4,5}N_{4,5}N_{4,5}$ Auger and $3d$ photoemission spectra (Al $K\alpha$, $h\nu = 1487$ eV), did not detect an increased Sb concentration at the immediate surface. This may result from the insufficient depth resolution at the kinetic energies involved ($\sim 400-500$ eV in AES and ~ 1 keV in XPS), which we have demonstrated by noting the dependence on E_p of the ELS of heavily oxidized samples.

ACKNOWLEDGMENTS

We are very grateful to E. M. Swiggard for providing the large quantity of single-crystal InSb used in these experiments.

[1] C. Wei, K. L. Wang, E. A. Taft, J. M. Swab, M. D. Gibbons, W. E. Davern, and D. M. Brown, IEEE Trans. Electron Devices ED-27, 170 (1980).

[2] J. D. Langan, Ph.D. thesis, University of California at Santa Barbara, 1979 (unpublished). Available from University Microfilms, Ann Arbor, Michigan, Order No. 80-19842.

[3] A. U. MacRae and G. W. Gobeli, J. Appl. Phys. 35, 1629 (1964).

[4] J. T. Grant and T. W. Haas, J. Vac. Sci. Technol. 8, 94 (1971).

[5] E. W. Kreutz, E. Rickus, and N. Sotnik, Thin Solid Films 42, 175 (1977).

[6] E. W. Kreutz, E. Rickus, and N. Sotnik, Appl. Surf. Sci. 3, 297 (1979).

[7] R. J. Meyer, C. B. Duke, A. Paton, J. L. Yeh, J. C.

Tsang, A. Kahn, and P. Mark, Phys. Rev. B 21, 4740 (1980).
[8]D. E. Eastman and J. L. Freeouf, Solid State Commun. 13, 1815 (1973).
[9]D. E. Eastman, W. D. Grobman, J. L. Freeouf, and M. Erbudak, Phys. Rev. B 9, 3473 (1974).
[10]C. J. Vesely and D. L. Kingston, Phys. Status Solidi B 61, 337 (1974).
[11]L. Ley, R. A. Pollak, F. R. McFeely, S. P. Kowalczyk, and D. A. Shirley, Phys. Rev. B 9, 600 (1974).
[12]R. G. Copperthwaite, O. A. Kunze, J. Lloyd, J. A. Neely, and W. Tuma, Z. Naturforsch. 33A, 523 (1978).
[13]H. Iwasaki, Y. Mizokawa, R. Nishitani, and S. Nakamura, Jpn. J. Appl. Phys. 17, 1925 (1978); 18, 1525 (1979); Surf. Sci. 86, 811 (1979).
[14]P. Legare, L. Hilaire, and G. Maire, J. Microsc. Spectrosc. Electron. 5, 771 (1980).
[15]R. P. Vasquez and F. J. Grunthaner, J. Vac. Sci. Technol. 19, 431 (1981); J. Appl. Phys. 52, 3509 (1981).
[16]E. W. Kreutz, E. Rickus, and N. Sotnik, Surf. Sci. 68, 392 (1977).
[17]C. W. Wilmsen, J. Vac. Sci. Technol. 19, 279 (1981).
[18]G. Margaritondo, J. E. Rowe, C. M. Bertoni, C. Calandra, and F. Manghi, Phys. Rev. B 20, 1538 (1979).
[19]J. van Laar, A. Huijser, and T. L. van Rooy, J. Vac. Sci. Technol. 14, 894 (1977).
[20]A. Huijser, J. van Laar, and T. L. van Rooy, Surf. Sci. 62, 472 (1977).
[21]J. D. Joannopoulos and M. L. Cohen, Phys. Rev. B 10, 5075 (1974).
[22]M. Nishida, Phys. Status Solidi B 99, K39 (1980).
[23]M. Schmeits, A. Mazur, and J. Pollmann, Solid State Commun. 40, 1081 (1981).
[24]D. E. Eastman and J. L. Freeouf, Phys. Rev. Lett. 34, 1624 (1975).
[25]E. W. Kreutz, E. Rickus, P. Schroll, and N. Sotnik, Surf. Sci. 86, 794 (1979).
[26]E. W. Kreutz, E. Rickus, and N. Sotnik, Surf. Sci. 95, 257 (1980).
[27]E. W. Kreutz, E. Rickus, and N. Sotnik, Appl. Surf. Sci. 6, 497 (1980).
[28]H. Lüth, M. Büchel, R. Dorn, M. Liehr, and R. Matz, Phys. Rev. B 15, 865 (1977).
[29]M. Liehr and H. Lüth, J. Vac. Sci. Technol. 16, 1200 (1979).
[30]E. W. Kreutz, Phys. Status Solidi A 56, 687 (1979).
[31]M. Büchel and H. Lüth, Phys. Status Solidi B 94, K155 (1979).
[32]J. A. R. Sampson, *Techniques of Vacuum Ultraviolet Spectroscopy* (Wiley, New York, 1967), p. 130.
[33]V. M. Bermudez and V. H. Ritz, Appl. Opt. 17, 547 (1978).
[34]V. M. Bermudez, Opt. Commun. 23, 413 (1977); 24, 123(E) (1978).
[35]V. M. Bermudez, Surf. Sci. 74, 548 (1978); 94, 29 (1980).
[36]P. Pianetta, I. Lindau, C. M. Garner, and W. E. Spicer, Phys. Rev. B 18, 2792 (1978).
[37]P. Pianetta, I. Lindau, P. E. Gregory, C. M. Garner, and W. E. Spicer, Surf. Sci. 72, 298 (1978).
[38]H. R. Philipp and H. Ehrenreich, in *Semiconductors and Semimetals,* edited by R. K. Willardson and A. C. Beer (Academic, New York, 1967), Vol. 3, p. 93.
[39]H. J. Mattausch and D. E. Aspnes, Phys. Rev. B 23, 1896 (1981).
[40]S. Zimmermann, J. Phys. C 9, 2643 (1976).
[41]S. Singh and E. B. Pattinson, in *Proceedings of the Seventh International Vacuum Congress and Third International Conference on Solid Surfaces* (R. Dombrozemsky *et al.,* Vienna, 1977), p. 2367.
[42]J. Olivier, P. Faulconnier, and R. Poirier, J. Appl. Phys. 51, 4990 (1980).
[43]D. E. Eastman, T. C. Chiang, P. Heimann, and F. J. Himpsel, Phys. Rev. Lett. 45, 656 (1980).
[44]P. W. Chye, C. Y. Su, I. Lindau, C. M. Garner, P. Pianetta, and W. E. Spicer, Surf. Sci. 88, 439 (1979).
[45]W. Gudat and D. E. Eastman, J. Vac. Sci. Technol. 13, 831 (1976).
[46]D. E. Aspnes and A. A. Studna, Appl. Phys. Lett. 39, 316 (1981).
[47]R. Matz, and H. Lüth, Appl. Phys. 18, 123 (1979).
[48]F. Meyer, Surf. Sci. 56, 37 (1976).
[49]F. Lukeš, Surf. Sci. 49, 344 (1975).
[50]M. Cardona, K. L. Shaklee, and F. H. Pollak, Phys. Rev. 154, 696 (1967).
[51]G. B. Blanchet and P. J. Stiles, Phys. Rev. B 21, 3273 (1980).
[52]G. B. Blanchet, P. J. Estrup, and P. J. Stiles, Phys. Rev. B 23, 3655 (1981).
[53]I. Lindau, P. Pianetta, W. E. Spicer, P. E. Gregory, C. M. Garner, and P. W. Chye, J. Electron Spectrosc. Relat. Phenom. 13, 155 (1978).
[54]C. D. Wagner, L. E. Davis, and W. M. Riggs, Surf. Interface Anal. 2, 53 (1980).
[55]T. P. Smirnova, A. N. Golubenko, N. F. Zacharchuk, V. I. Belyi, G. A. Kokovin, and N. A. Valisheva, Thin Solid Films 76, 11 (1981).